Asymmetric spin-orbit coupling in single-walled carbon nanotubes

Jian Zhou,[1,2] Qifeng Liang,[3] and Jinming Dong[2,*]

[1]*Department of Material Science and Engineering and National Laboratory of Solid State Microstructures, Nanjing University, Nanjing 210093, People's Republic of China*

[2]*Department of Physics and National Laboratory of Solid State Microstructures, Group of Computational Condensed Matter Physics, Nanjing University, Nanjing 210093, People's Republic of China*

[3]*Department of Physics, Shaoxing University, Shaoxing 312000, People's Republic of China*

(Received 28 April 2009; published 21 May 2009)

The spin-orbit coupling (SOC) of single-walled carbon nanotube (SWNT) has been studied using both the first-principles and tight-binding (TB) methods. It is found that the curvature-induced σ-π coupling in the SWNTs always causes a more strong SOC in their π bonding states than their π^* antibonding ones. And a microscopic mechanism has been proposed to satisfactorily explain the experimental observation that the SOC-induced band splitting in the SWNTs is different for electrons and holes [Nature (London) **452**, 448 (2008)], which cannot be accounted for by the present theories. Finally, a SOC's family behavior of the SWNTs is also found, showing that their SOC depends on both the tube's chirality and family type.

DOI: 10.1103/PhysRevB.79.195427 PACS number(s): 73.22.−f, 71.15.Mb, 71.70.Ej, 73.63.Fg

I. INTRODUCTION

Carbon nanotube (CNT), a typical quasi-one-dimensional material, has attracted much attentions of researchers since its discovery[1] due to its unique geometrical, electronic, and optical properties.[2] A lot of theoretical and experimental works have been done on its electronic[3] and optical[4] properties because of its great potential applications in future nanoelectronic and optical devices.

On the other hand, CNT is also a promising candidate for spin-based applications,[5–7] such as spin-qubits[8] and spintronics,[9] because its spin-orbit coupling (SOC) was thought to be weak, making it possible to transfer spin information over a long distance in it. Up to now, there are several theoretical studies on the single-walled carbon nanotube (SWNT) SOC, using the tight-binding (TB) method,[10–12] which considered the SWNT's curvature is quite important, compared with the flat graphene. For example, Huertas-Hernando *et al.*[11] derived a continuum model for the effective spin-orbit interaction in curved graphenes, fullerenes, and nanotubes, showing that the local curvature in them can induce an additional effective SOC of the π electrons due to mixing of their σ and π bands, which is larger than that in the perfectly flat graphene.

It is well known that the SWNT's electronic ground states are fourfold degenerate due to independent spin and orbital symmetries, which can be lifted by an applied magnetic field parallel to the tube axis. Very recently, however, Kuemmeth *et al.*[13] surprisingly found in their experiment that the fourfold degenerate and electron-hole symmetry are broken even in the absence of a magnetic field. They measured the SOC-induced band splitting Δ_{SO} in a clean CNT with its diameter of $d=5$ nm and found that it is different for electrons and holes with $\Delta_{SO}=0.37$ meV for electron and $\Delta_{SO}=0.21$ meV for hole, which are much larger than those of the π band in the graphene, showing a strong spin-orbit interaction in the CNTs than previously thought.

The authors of Ref. 13 thought that their experimental results are mostly consistent with the theoretical calculations except the unsymmetric spin-orbit splittings for electrons and holes, which could not be explained by current theory. Therefore, it is very interesting and important to ask what is the reason to cause the different Δ_{SO} for electrons and holes and why the present theories could not account for it.

In this paper, we will use the first-principles calculations and auxiliary TB method to study the SOC in SWNTs with different diameters and chiral angles, paying more attention to the difference between their SOC effects for electron and hole.

II. COMPUTATIONAL DETAIL

The SWNT's SOC has been calculated by the density-functional theory in VASP (Refs. 14 and 15) code, in which the projected augmented wave (PAW) method[16,17] and the Ceperley-Alder-type exchange correlation are used. And the $2s$ and $2p$ orbitals of the carbon atom are treated as valence ones. A large unit cell is used to simulate the isolated SWNT, making the closest distance between two adjacent SWNTs to be 10 Å. Both of the atomic positions and the lattice constant along tube axis are optimized. Since the Δ_{SO} is quite small in the carbon-based materials, the highly accurate parameters and a dense k mesh have to be used in the calculations. For example, a uniform grid of $1\times1\times35$ k points is used for zigzag SWNTs and $1\times1\times60$ k points for armchair tubes. Once the optimized structure is obtained, an even much denser k mesh would be used to calculate the band structure with and without the SOC. By comparing the two band structures, the SOC-induced band splitting can be obtained. The four-electron TB method is also used, and the related parameters are the same as those in Ref. 11. It is found that the obtained results by both the TB and first-principles methods are well consistent to each other.

The graphene's SOC-induced band splitting is first calculated and found to be about 9.4 meV at its Γ point and about 10^{-3} meV at its K point (Dirac point). They are in good agreement with Yao *et al.*'s results.[18]

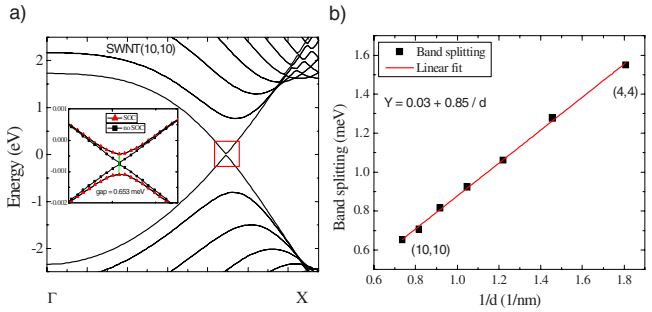

FIG. 1. (Color online) (a) Band structure of armchair (10,10) SWNT. Its Dirac point is indicated by a small red square (Fermi energy is set to 0). The inset shows its band structure near Dirac point with and without the SOC, denoted by the red triangle and black square, respectively. (b) Δ_{SO} vs the inverse diameter $(1/d)$ of the armchair SWNTs with different diameters from (4,4) to (10,10). The red line is a linear fit to the splittings.

III. RESULTS AND DISCUSSIONS

A. Armchair SWNT

It is well known that all the armchair SWNTs are metallic with their Dirac point located just on the Fermi level. Figure 1(a) shows the band structure of a (10,10) SWNT. It can be seen clearly from its inset that a SOC-induced energy gap appears at very near the Dirac point, which is found to be about 0.653 meV, much larger than that in graphene. This is because the π-electron states near its Fermi level contain some composition of σ electrons due to σ-π coupling caused by its tube's curvature, and the σ electrons in graphene can have a rather large Δ_{SO}, reaching to about 9.4 meV. Therefore, it is expected that this kind of Δ_{SO} can be larger in the small diameter SWNTs but never be larger than 9.4 meV.

We have also calculated the Δ_{SO} for different diameter armchair (n,n) SWNTs with $n=4$ to 10, shown in Fig. 1(b). It is found that the Δ_{SO} of (4,4) tube is 1.55 meV, about two times larger than that of (10,10) SWNT, which is obviously caused by the larger curvature effect in the smaller diameter tubes. The SOC-induced energy gap in the armchair SWNTs is found to be well proportional to their inverse diameter: $\Delta_{SO} \approx 0.85$ meV$/d$, where the diameter's unit is nm.

It is found that the armchair SWNT's Δ_{SO} can appear only at the very vicinity of their Dirac points, and so a small deviation from their Dirac points can avoid the SOC effect, making the armchair SWNTs still to be more suitable for spin information transfer over a long distance.

B. Zigzag SWNT

However, the SWNT used in the experiment of Ref. 13 is semiconducting. So, we further study the zigzag $(n,0)$ SWNTs, which are all semiconductors based upon the first-principles calculations. In the experiment,[13] the Δ_{SO} for electrons and holes, measured by the one-electron and one-hole excitation spectra, corresponds to that for the lowest unoccupied molecular orbital (LUMO) states and the highest occupied molecular orbital (HOMO) ones, respectively. Taking as an example, we calculate the band structure of a (15,0) tube and its Δ_{SO} nearby Γ point in the LUMO and HOMO states,

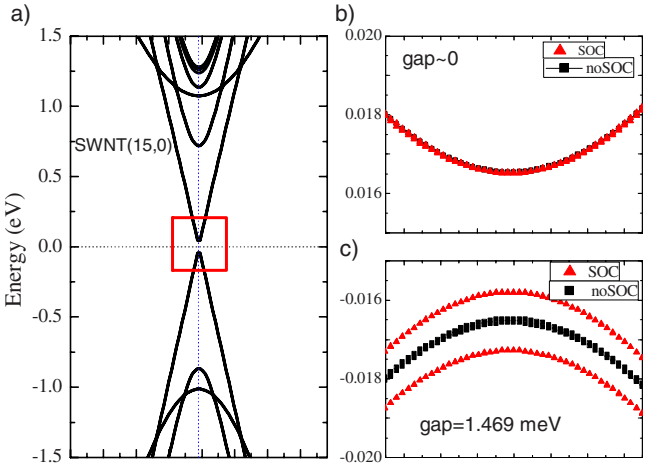

FIG. 2. (Color online) (a) Band structure of the zigzag (15,0) SWNT. The SOC-induced band splitting in: (b) its LUMO states and (c) its HOMO ones. Here, the red triangle and black square denote the case with and without SOC, respectively.

which are shown in Fig. 2. It is clearly seen from Fig. 2 that the Δ_{SO} in its LUMO state is almost 0, while it is about 1.469 meV in the HOMO state, showing an obvious difference between the SOC-induced band splittings for electrons and holes.

All the calculated Δ_{SO} for electrons and holes in different diameter zigzag $(n,0)$ SWNTs from $n=11$ to 22 are given in Fig. 3, from which it can be seen that the splitting is indeed different for electrons and holes in each zigzag tube, but the splitting for electrons is not always larger than that for holes. In fact, it is found for each zigzag tube that among the band splittings of electrons and holes, there is always one to be rather large (about 1 meV), and the other is almost 0. The inset of Fig. 3 gives the ratio β of the σ electron composition to the total one in the electron and hole states due to σ-π coupling. We can see from the inset that the variation in β with tube diameter in the electron and hole states is almost

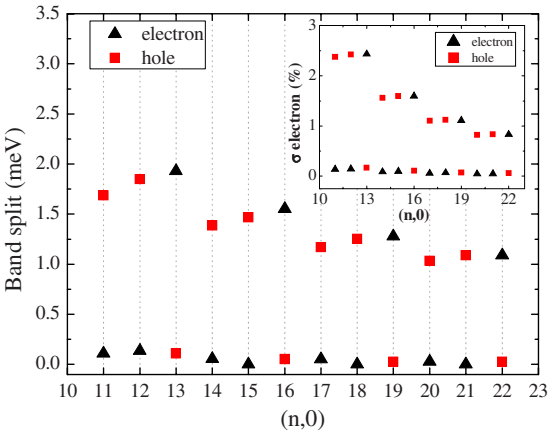

FIG. 3. (Color online) The SOC-induced band splitting in the HOMO (or hole) and LUMO (or electron) states of different diameter zigzag SWNTs from (11,0) to (22,0). And the inset shows the ratio β of the σ-electron composition to the total one in both the states. Here, black triangle and red square denote the splitting (or the ratio) for electrons and holes, respectively.

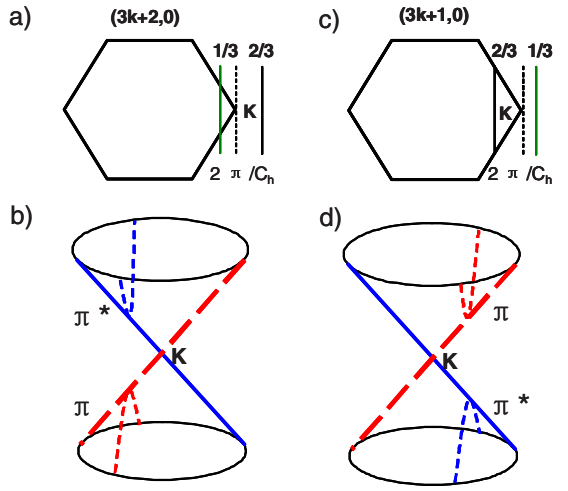

FIG. 4. (Color online) (a) The first Brillouin zone and (b) energy dispersion around K point of type-I zigzag $(3\ k+2,0)$ tubes, where k is an positive integer. (c) and (d) are the same as (a) and (b), respectively, but now for type-II zigzag $(3\ k+1,0)$ tubes. In (a) and (c), the distance between two parallel lines around K point is equal to $2\pi/C_h$ with C_h the SWNT's circumference. The thick red dashed and blue solid lines denote the π-bonding and π^* antibonding states, respectively.

exactly the same as that of the Δ_{SO}, confirming the σ electron plays an important role in causing SWNT's SOC.

It is very interesting to note from Fig. 3 that the Δ_{SO} of electrons or holes strongly depends on the tube index n of zigzag $(n,0)$ SWNTs. In addition to an ordinary decrease in the Δ_{SO} with the index n, there exists an another obvious modulation of Δ_{SO}, superimposed on its general decrease, which has a period of 3. That means for the metallic and type-I zigzag $(n,0)$ tubes (with $2n$ mod $3=0$ or 1, respectively), their hole's Δ_{SO} is much larger than that of electron. While for the type-II zigzag ones (with $2n$ mod $3=2$), their electron's Δ_{SO} becomes much larger than that of hole. This behavior of the SOC is very similar to the family behavior of SWNT's electronic structures, which can be easily observed in the optical transitions of SWNTs.[19] Therefore, we also name this Δ_{SO} behavior as a kind of family behavior.

It is important to ask why such a big difference exists between the Δ_{SO} for electrons and holes and what is the reason to cause the SOC's family behavior in SWNTs. We have made a four-electron TB calculation on these problems and obtained results not only confirm the above first-principles ones but also give us a clear physical explanation of these phenomena.

The Brillouin zones and the band structures around K point of type-I and type-II zigzag SWNTs are given schematically in Fig. 4 when the curvature effect is neglected. Since we now concern mainly the HOMO and LUMO states, only those bands nearest to Fermi level (K point) are taken into account [the left vertical solid line in Fig. 4(a) and the right vertical solid line in Fig. 4(c)]. It is well known that for type-I zigzag tubes, their energy band nearest to K point lies at the left side of K point with a distance of $\Delta K=-\frac{1}{3}\frac{2\pi}{C_h}$, while for type-II ones, it lies at the right side of K point with a distance of $\Delta K=+\frac{1}{3}\frac{2\pi}{C_h}$. For both the type-I and type-II zigzag SWNTs, the eigenenergies of their bonding (π) and antibonding (π^*) states are given as follows:

$$E(\pi) = -V_{pp\pi}\Delta K a_{cc}/2,$$

$$E(\pi^*) = V_{pp\pi}\Delta K a_{cc}/2, \tag{1}$$

where $V_{pp\pi}=-2.24$ eV and a_{cc} is the C-C bond length in SWNTs (about 1.42 Å). And both of their π and π^* states contain no any composition of σ electrons, i.e., $\beta(\pi)=0$ and $\beta(\pi^*)=0$.

Now, we include the curvature effect in SWNTs, which can induce the σ-π coupling. It is known that for larger diameter SWNTs, the curvature effect could only cause a small σ-π coupling, leading to a small perturbation to the band structures and bonding π and antibonding π^* states. Under this approximation, our four-electron TB calculations found that

$$\beta(\pi) = 0.097\ 52\theta^2 + 0.313\ 62\theta^2\Delta K\sqrt{3}a_{cc}/2,$$

$$\beta(\pi^*) = 0.024\ 24\theta^2 + 0.052\ 06\theta^2\Delta K\sqrt{3}a_{cc}/2, \tag{2}$$

where θ is the angle between two p_z states on the two nearest-neighbor carbon atoms caused by the curvature effect. And the eigenenergies of the π and π^* states are almost not changed, which are still expressed by Eq. (1).

It is clearly seen from Eq. (2) that the bonding π state has always more composition of σ electrons due to the σ-π coupling than the antibonding π^* state, which makes the former always to have the larger Δ_{SO} than the latter for the same zigzag SWNTs. That means the unsymmetric SOC for the electrons and holes is an intrinsic property of zigzag SWNTs, which is caused by both of the curvature effect and the wave function symmetries of their LUMO and HOMO states. More importantly, however, we have further found that the electron's SOC is not always larger than that of the holes, as found in the experiment.[13] In fact, it is known from Eq. (1) that when $\Delta K<0$, corresponding to type-I zigzag tubes, we have $E(\pi)<E(\pi^*)$, and in this case, the $\pi(\pi^*)$ state is clearly the hole (electron) state, called in the experiment of Ref. 13, as shown in Fig. 4(b). Therefore, for type-I zigzag SWNTs, the hole's SOC must be greatly larger than the electron's one. Similarly, when $\Delta K>0$ for type-II zigzag tubes, we have $E(\pi)>E(\pi^*)$, leading to an opposite situation to that for type-I ones, i.e., the $\pi(\pi^*)$ state corresponds now to the electron (hole) state, as shown in Fig. 4(d). And so, for type-II zigzag tubes, the electron's SOC must be greatly larger than the hole's one.

As for the metallic zigzag SWNTs, it is well known from both TB calculation and the first-principles method that the curvature effect would induce a small gap at their K point, and similar to type-I zigzag tubes, their HOMO state (the hole one) is the π-bonding state and LUMO state (the electron one) is the π^* antibonding state. Thus, their hole's SOC is much larger than that of the electron, which is the same as that for type-I zigzag tubes. Therefore, the approximate analytic TB result confirms our first-principles calculations, shown in Fig. 3.

TABLE I. Δ_{SO} for electrons and holes of the chiral SWNTs (n,m) with different chiral angles and family types.

	Electron (meV)	Hole (meV)	$(2n+m)$mod 3	Degree (deg)
(8,1)	3.031	0.465	2	5.8
(8,2)	0.148	2.154	0	10.9
(8,3)	0.274	1.432	1	15.3
(8,4)	1.879	0.076	2	19.1
(8,5)	0.388	1.249	0	22.4
(8,6)	0.711	0.809	1	25.3
(8,7)	1.039	0.457	2	27.8
(7,6)	1.252	0.482	2	27.4
(9,8)	0.885	0.430	2	28.0
(10,9)	0.769	0.405	2	28.2

Finally, it is found from Eq. (2) that the first θ^2 term makes the SOC of the zigzag tubes decreases with increase in their diameter, while the second $\theta^2\Delta K$ term presents a modulation of the SOC with a period of 3. Since ΔK can be equal to $+\frac{1}{3}\frac{2\pi}{C_h}$, $-\frac{1}{3}\frac{2\pi}{C_h}$, or 0, depending on the tube index n, which is caused by the SWNT's family behavior, we can conclude that the SOC's family behavior in the zigzag SWNTs comes directly from the SWNT's family behavior, which, we hope, will be possibly proved by future experiments.

C. Chiral SWNT

We should emphasize that the above obtained conclusions for zigzag SWNTs, e.g., the unsymmetric SOC for electrons and holes, and the SOC's family behavior, are found to be universal, which can be extended to the chiral SWNTs. In order to see it more clearly, we have used the four-electron TB method to study the SOC effects of chiral SWNTs with different chiral angles and family types because the unit cell of chiral SWNTs is too big to use the *ab initio* calculations. The obtained results are given in Table I, from which it is clearly seen that the Δ_{SO} for electrons and holes in chiral SWNTs is not symmetric either, and the same SOC's family behavior can be found too. For example, for metallic or type-I semiconducting chiral (n,m) SWNTs with their $(2n+m)$mod $3=0$ or 1, their hole's Δ_{SO} is larger than that for electrons. But, for type-II semiconducting chiral SWNTs with their $(2n+m)$ mod $3=2$, their electron's Δ_{SO} is larger than that for their holes. Therefore, it is obvious that all the obtained results are universal, which are suitable for both chiral and zigzag SWNTs.

Finally, it is interesting to note that the SOC for electrons is observed in the experiment[13] to be larger than that for holes. Based upon our calculation results, we believe that the SWNT sample used in the experiment is a type-II semiconducting SWNT. Furthermore, it can be found from Table I that for the same family of chiral (n,m) SWNTs, e.g., the type-II SWNTs, the ratio of electron's Δ_{SO} to hole's one is quite different for the SWNTs with different chiral angles. For example, the ratio value for (10,9) chiral SWNT with its chiral angle of 28.2° is found to be about 1.9, which is very close to the experimental value (about 1.8). So, we believe that the SWNT used in the experiment is an armchairlike type-II chiral tube, i.e., its chiral angle is close to 30°.

IV. CONCLUSION

In summary, we have calculated the SOCs in both the chiral and achiral SWNTs by the first-principles and four-electron TB methods. Our obtained results have presented a reasonable interpretation of the experimental observation that the SOC-induced band splitting Δ_{SO} in the SWNTs are unsymmetric for electrons and holes, which is caused by both the curvature-induced σ-π coupling and the SWNT's band dispersions, leading to different proportions of the σ electrons in their π and π^* states because the σ electron plays a crucial role in causing the Δ_{SO}, as shown in graphene.

We have further found an obvious SOC's family behavior for the zigzag and chiral SWNTs: (1) in the metallic and type-I SWNTs, the Δ_{SO} for holes is larger than that for electrons; (2) while in type-II ones, the situation is reversed, i.e., the Δ_{SO} for electrons is larger than that for holes; (3) The ratio of electron's Δ_{SO} to hole's one is found to depend strongly on the SWNT's chiral angle, all of which could be proved by future experiments.

Finally, it is found that the Δ_{SO} in armchair SWNTs appears only near their Dirac point, which makes them still possibly more suitable for transporting spin information. Our obtained results will be able to help ones to understand deeply the SWNT's SOC, especially in its applications in the field of spintronics and quantum informations.

ACKNOWLEDGMENTS

This work was supported by the Natural Science Foundation of China under Grant No. 10874067 and also from a Grant for State Key Program of China through Grants No. 2004CB619004 and No. 2006CB921803. J.Z. was also supported by the China Postdoctoral Science Foundation funded project and the Jiangsu Planned Projects for Postdoctoral Research Funds.

*Corresponding author: jdong@nju.edu.cn

[1] S. Iijima, Nature (London) **354**, 56 (1991).

[2] M. S. Dresselhaus, G. Dresselhaus, and Ph. Avouris, *Carbon Nanotubes: Synthesis, Structure, Properties, and Applications* (Springer-Verlag, Berlin, 2001).

[3] J. C. Charlier, X. Blase, and S. Roche, Rev. Mod. Phys. **79**, 677 (2007).

[4] S. M. Bachilo, M. S. Strano, C. Kittrell, R. H. Hauge, R. E.

Smalley, and R. B. Weisman, Science **298**, 2361 (2002).
[5] K. Tsukagoshi, B. W. Alphenaar, and H. Ago, Nature (London) **401**, 572 (1999).
[6] N. Tombros, S. J. van der Molen, and B. J. van Wees, Phys. Rev. B **73**, 233403 (2006).
[7] L. E. Hueso, J. M. Pruneda, V. Ferrari, G. Burnell, J. P. Valdés-Herrera, B. D. Simons, P. B. Littlewood, E. Artacho, A. Fert, and N. D. Mathur, Nature (London) **445**, 410 (2007).
[8] K. C. Nowack, F. H. L. Koppens, Y. V. Nazarov, and L. M. K. Vandersypen, Science **318**, 1430 (2007).
[9] S. Sahoo, T. Kontos, J. Furer, C. Hoffmann, M. Gräber, A. Cottet, and C. Schönenberger, Nat. Phys. **1**, 99 (2005).
[10] T. Ando, J. Phys. Soc. Jpn. **69**, 1757 (2000).
[11] D. Huertas-Hernando, F. Guinea, and A. Brataas, Phys. Rev. B **74**, 155426 (2006).
[12] L. Chico, M. P. López-Sancho, and M. C. Muñoz, Phys. Rev. Lett. **93**, 176402 (2004).
[13] F. Kuemmeth, S. IIani, D. C. Ralph, and P. L. McEuen, Nature (London) **452**, 448 (2008).
[14] G. Kresse and J. Hafner, Phys. Rev. B **48**, 13115 (1993).
[15] G. Kresse and J. Furthmüller, Comput. Mater. Sci. **6**, 15 (1996).
[16] P. E. Blöchl, Phys. Rev. B **50**, 17953 (1994).
[17] G. Kresse and D. Joubert, Phys. Rev. B **59**, 1758 (1999).
[18] Y. Yao, F. Ye, X. L. Qi, S. C. Zhang, and Z. Fang, Phys. Rev. B **75**, 041401(R) (2007).
[19] G. G. Samsonidze, R. Saito, N. Kobayashi, A. Grüneis, J. Jiang, A. Jorio, S. G. Chou, G. Dresselhaus, and M. S. Dresselhaus, Appl. Phys. Lett. **85**, 5703 (2004).